JOURNAL OF CRYSTAL GROWTH

Journal of Crystal Growth 191 (1998) 39–43

Growth and characterization of InAs-rich GaInAsSb alloys on GaSb substrates by MOCVD

Yongqiang Ning*, Tianming Zhou, Baolin Zhang, Hong Jiang,
Shuwei Li, Guang Yuan, Yuan Tian, Yixin Jin

Changchun Institute of Physics, Chinese Academy of Sciences, 1 Yan'an Road, Changchun, Changchun 130021, People's Republic of China

Received 13 May 1997; accepted 7 November 1997

Abstract

MOCVD growth and characterization of InAs-rich GaInAsSb on GaSb substrates was investigated. High quality mirror-like surfaces with a minimum lattice mismatch of 0.4% was obtained. The surface of InAs-rich GaInAsSb epilayer shows morphological features much different from that of GaSb-rich films. Solid compositions of InAs-rich films were dependent on growth temperature. InAs-rich GaInAsSb shows n-type conduction, which is the opposite of GaSb-rich samples. A room temperature electron mobility of 5000 $\mathrm{cm^2/V\cdot s}$ with electron concentration of $3.6\times10^{17}\ \mathrm{cm^{-3}}$ was obtained. © 1998 Elsevier Science B.V. All rights reserved.

PACS: 61.50.C; 81.10.B; 73.60.F

Keywords: MOCVD; GaInAsSb; InAs-rich; Surface morphology; Electrical property

1. Introduction

III–V antimonide compounds are attracting great interest for their applications, such as optical communications, environmental protection, remoting sensing of atmosphere and infrared focal plane arrays for imaging. The room temperature band gaps of Sb-containing materials cover the extremely wide range from 1.43 to 0.1 eV, corresponding to 0.9–12 μm. Lattice-matched to GaSb substrates, the energy band gap varies between 1.7 and 4.3 μm. GaInAsSb materials are also of interest due to the miscibility gap with a critical temperature estimated to be 1467°C [1]. The nonequilibrium growth by MOCVD and MBE can conquer the difficulty of phase separation in the miscibility gap [2–6]. The growth of GaInAsSb alloys have been reported by LPE (liquid phase epitaxy) [7,8], MOCVD (metalorganic chemical vapor deposition) [2–5], MBE (molecular beam epitaxy) [6,9] and LPEE (liquid phase electroepitaxy) [10,11]. Photodiodes [5,12–14] and lasers [15–17] fabricated from GaInAsSb materials have also been demonstrated. Most of the epitaxial growth of

---

*Corresponding author. Fax: + 86 431 5955378; e-mail: snmocvd@public.cc.jl.cn.

PII S0022-0248(97)00855-5

materials and the fabrication of devices was performed for alloys in the GaSb-rich end of the composition range. In this end the epilayers are p-type. Pyramids and other defects were likely to occur on the surface of GaSb, GaSb-rich GaInSb and GaInAsSb epilayers [5,12,18–20]. Although there has been many reports on GaInAsSb alloys, to my knowledge, there has been no detailed study to date on the growth property of InAs-rich GaInAsSb alloys by MOCVD. In this work,we report the growth of GaInAsSb alloys grown on GaSb substrates by MOCVD, with compositions on the InAs-rich end.

2. Experimental procedure

The epitaxial growth was performed in a horizontal, atmospheric MOCVD pressure reactor. The precursors were trimethylgallium (TMGa), trimethylindium (TMIn), trimethylantimony (TMSb) and 10% arsine diluted by hydrogen. The source temperatures for TMGa,TMIn and TMSb were −12°C, 17°C, and −10°C, respectively. The carrier gas was Pd-purified H_2 at a total flow of 3 l/min (1 0 0)-oriented, Te-doped GaSb and high resistivity GaAs were used as substrates. The substrates were first cleaned by degreasing in organic solvents and deionized water. Then they were chemically etched. For GaSb substrates, the etchant used was a mixed solution of nitric acid, hydrochloric acid and ice-acetic acid ($HNO_3 : HCl : CH_3COOH = 0.2 : 2 : 10$) for 10 min. The etchant for GaAs was the standard chemical etching solution ($H_2SO_4 : H_2O : H_2O_2 = 5 : 1 : 1$). After etching, the substrates were rinsed with deionized water, blown dry with filtered nitrogen and loaded into the reaction chamber.

GaSb and GaAs substrates were protected from decomposing by TMSb and arsine sources before reaching the growth temperature. The growth parameters, such as growth temperature and mole ratios of the input sources, were optimized to decrease the lattice mismatch between the GaInAsSb epilayer and the GaSb substrate. Table 1 presents the optimized growth parameters of InAs-rich $Ga_{1-x}In_xAs_ySb_{1-y}$ grown on GaSb substrates. Under these conditions the solid compositions of the epilayers were on the InAs-rich end with $x > 0.7$, and $y > 0.7$. The thicknesses of the epilayers are about 1–3 μm.

Table 1
Growth conditions of InAs-rich $Ga_{1-x}In_xAs_ySb_{1-y}$ films on GaSb substrates

Growth temperature (°C)	570–620
TMGa flux (mol/min)	$(1–1.5) \times 10^{-6}$
TMIn flux (mol/min)	$(0.8–3) \times 10^{-5}$
TMSb flux (mol/min)	$(0.8–3) \times 10^{-5}$
AsH_3 flux (mol/min)	$(3–5) \times 10^{-5}$
total H_2 flux (l/min)	3
III/V mole ratio	0.2–0.4
Ga/III mole ratio	0.05–0.15
Sb/V mole ratio	0.1–0.3

The surface morphologies were examined by means of optical microscopy and scanning electron microscopy (SEM). The solid composition and lattice mismatch were measured by electron microprobe analysis and X-ray diffraction, respectively. X-ray diffraction was also used to evaluate the crystalline quality of the epilayers. Standard Hall measurements were performed to determine the electrical properties of the GaInAsSb epilayers grown on semi-insulating GaAs substrates.

3. Results and discussion

3.1. X-ray diffraction

InAs-rich GaInAsSb epilayers of good quality were grown on GaSb substrates. The growth parameters used are presented in Table 1. The epilayers were mirror-like with smooth surfaces. The lattice mismatch between GaInAsSb and GaSb was about 1–2%. A minimum mismatch of 0.4% was achieved. Typical X-ray diffraction results for several samples of GaInAsSb/GaSb are shown in Fig. 1. These results show that the crystalline quality is good.

3.2. Solid composition

The solid composition of GaInAsSb was dependent on growth temperature. Figs. 2 and 3 show the

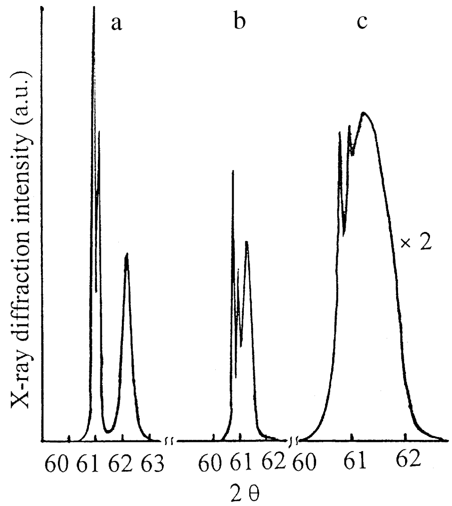

Fig. 1. X-ray diffraction of three InAs-rich $Ga_{1-x}In_xAs_ySb_{1-y}$/GaSb samples. (a) III/V ratio = 0.22, Ga/III ratio = 0.09, Sb/V ratio = 0.17, growth temperature $T = 600°C$, solid composition $x = 0.72$, $y = 0.78$, thickness $d = 1$ μm. (b) III/V ratio = 0.34, Ga/III ratio = 0.06, Sb/V ratio = 0.16, growth temperature $T = 570°C$, solid composition $x = 0.71$, $y = 0.72$, thickness $d = 2$ μm. (c) III/V ratio = 0.44, Ga/III ratio = 0.06, Sb/V ratio = 0.20, growth temperature $T = 600°C$, solid composition $x = 0.84$, $y = 0.81$, thickness $d = 3.5$ μm.

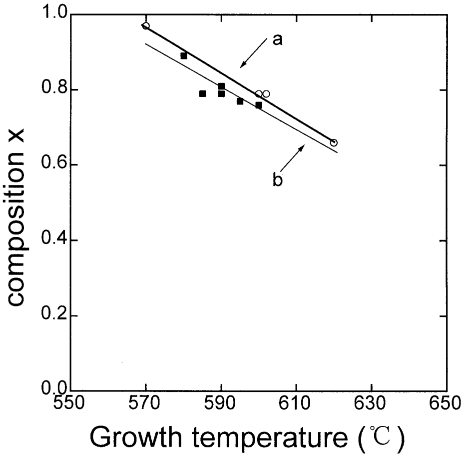

Fig. 2. Solid composition x of $Ga_{1-x}In_xAs_ySb_{1-y}$ versus growth temperature. (a) III/V = 0.36, Ga/III = 0.07, Sb/V = 0.17 and (b) III/V = 0.22, Ga/III = 0.13, Sb/V = 0.16.

temperature dependence of In composition x and As composition y, respectively. In Fig. 2, the GaInAsSb alloys were grown on GaSb substrates at temperatures between 570 and 620°C. The indium composition x decreased with increasing growth temperature. This phenomenon was often attributed to the difference of pyrolysis efficiency between TMGa and TMIn [21]. The pyrolysis temperature of TMGa is higher than that of TMIn, which pyrolyses completely at 500°C. In the range of 570–620°C, the pyrolysis efficiency of TMGa increases with increasing growth temperature, resulting in the decrease of indium composition in the epilayers.

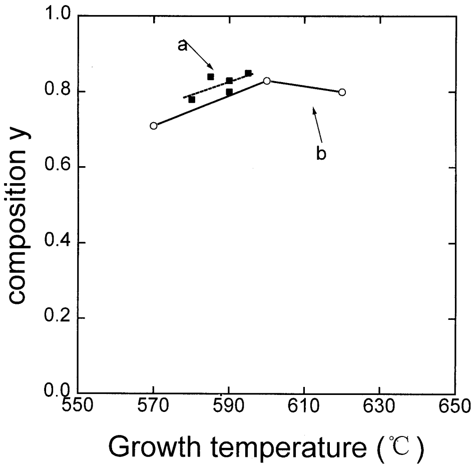

Fig. 3. Solid composition y of $Ga_{1-x}In_xAs_ySb_{1-y}$ versus growth temperature. (a) III/V = 0.22, Ga/III = 0.13, Sb/V = 0.16 and (b) III/V = 0.36, Ga/III = 0.07, Sb/V = 0.17.

Fig. 3 shows the unusual temperature dependence of As composition y in InAs-rich GaInAsSb alloys. In the range of 570–600°C, y increases with increasing growth temperature. This can be explained by the different pyrolysis efficiencies of TMSb and AsH_3 [3]. It is well known that TMSb is nearly completely pyrolysed above 500°C. On the other hand, the pyrolysis of AsH_3 is not complete and increases with increasing growth temperature [22]. The real ratio of As and Sb in vapor phase consequently increases, resulting in the increase of As composition y. Above 600°C, y decreased with increasing growth temperature. The reason for this tendency is not very clear. A possible explanation is that the decrease of y might be due to the stronger parasitic reaction between TMIn and AsH_3 in vapor phase when the growth temperature is increased [23].

3.3. Surface morphology

The detailed surface morphology was examined using optical microscopy and scanning electron microscopy. Fig. 4 shows several surface observations of InAs-rich GaInAsSb samples. As a comparison, GaSb-rich GaInAsSb film was also examined using the above techniques. Surface morphology observations demonstrate that the surface morphologies of InAs-rich GaInAsSb epilayers were much different from GaSb-rich GaInAsSb, as shown in Fig. 4. For GaSb-rich films, huge hillocks with the size of about 10 μm were observed on the surface. The pyramid-like hillocks have a rectangular base plane. The direction of the edges of the rectangular bottom is related to the tilt of the substrate. However, for InAs-rich samples, no such features were observed. The surface was mirror-like with very small hillocks on the surface. Such high quality surfaces without lots of pyramids would be beneficial for device fabrication. Previously reported results have shown that surface defects such as pyramids often occur in the growth of antimonide compounds such as GaSb [18,19], GaInSb [20] and GaInAsSb [5,12]. In other material growth such as GaAs,InP and GaInAs, no such features are observed. Considering the above results and the much different TMSb flux used for GaSb-rich and InAs-rich films, we believe that the presence of antimony has much to do with the occurrence of pyramids. For the growth of InAs-rich GaInAsSb films, the mole ratios of antimony versus group-V elements were chosen to be about 0.10–0.3 in our work, much lower than for GaSb-rich GaInAsSb. In this case, the surface morphology of InAs-rich GaInAsSb epilayers was then to a great extent determined by the incorporation of arsenic and group-III elements, avoiding the occurance of hillocks.

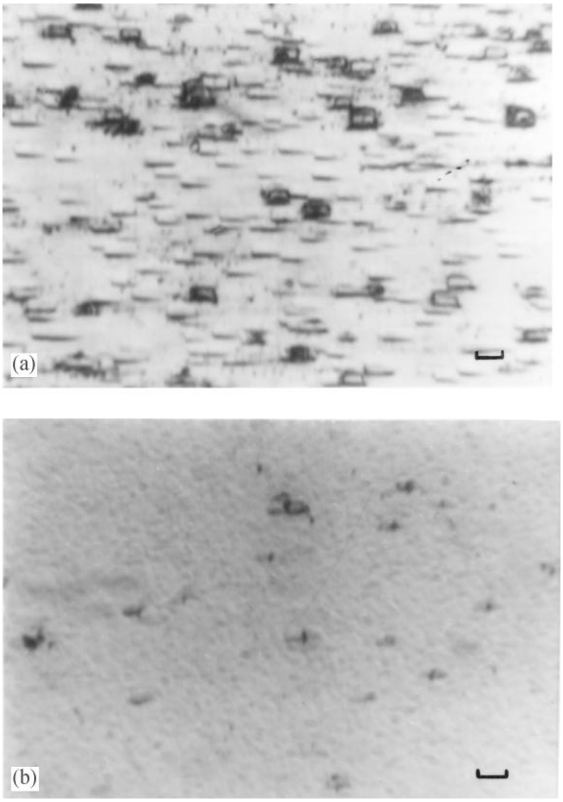

Fig. 4. Surface morphologies of GaSb-rich and InAs-rich $Ga_{1-x}In_xAs_ySb_{1-y}$/GaSb films, marker represents 10 μm (a) III/V ratio = 0.79, Ga/III ratio = 0.78, Sb/V ratio = 0.86, growth temperature $T = 640°C$, solid composition $x = 0.06$, $y = 0.10$, thickness $d = 1 μm$, lattice mismatch $\Delta a/a = 1\%$ and (b) III/V ratio = 0.22, Ga/III ratio = 0.13, Sb/V ratio = 0.16, growth temperature $T = 560°C$, solid composition = 0.80, $y = 0.83$, thickness $d = 3 μm$, lattice mismatch $\Delta a/a = 1.6\%$.

3.4. Electrical properties

The electrical properties of InAs-rich GaInAsSb deposited on semi-insulating GaAs substrates were measured using the Hall method. We observed that the type of conduction in InAs-rich films was n-type, the opposite of GaSb-rich samples. A room temperature electron mobility of 5000 $cm^2/V \cdot s$ and an electron concentration of 3.6×10^{17} cm^{-3} were obtained. The origin of p-type conduction of GaSb-rich GaInAsSb alloys was often attributed to native lattice defects (i.e. Sb vacancies), antisite defects (Ga atoms at Sb sites), defect complex ($V_{Ga}Ga_{Sb}$) [24,25]. Another possible explanation for p-type conduction might be that carbon occupys group-V element sites as an acceptor in the materials, as shown in OMVPE-GaAs [26]. In GaAs, GaSb and GaSb-rich GaInAsSb, the strong Ga–C bond forces carbon onto the group-V sublattice,and therefore carbon is an acceptor. For InAs and InAsSb the In–C bond is relatively weak and the result is n-type material with carbon on group-III sites [27]. This assumption could reasonably explain the n-type conduction of InAs-rich GaInAsSb in our work because the concentration of the In–C bond was much higher than that of the Ga–C bond.

According to our experimental results, we suggest that unintentionally doped GaInAsSb epilayers will show the lowest carrier concentration and the highest mobility when the effect of GaSb on the electrical conduction is comparable with that of InAs. This work is under way.

4. Conclusions

High quality InAs-rich $Ga_{1-x}In_xAs_ySb_{1-y}$ with compositions of $x > 0.7$, $y > 0.7$ were grown on GaSb substrates by atmospheric pressure MOCVD. The surfaces are smooth and mirror-like. The detailed surface morphology and electrical properties were investigated. Both of them were much different from those of GaSb-rich GaInAsSb films. The concentration of TMSb apparently greatly affects the surface morphology. An electron mobility of $5000\,\mathrm{cm^2/V \cdot s}$ with a concentration of $3.6 \times 10^{17}\,\mathrm{cm^{-3}}$ was achieved.

Acknowledgements

The authors were grateful to Jingxiu Jiang, Naikang Liu, Zhongjiu Ge for their assistance in measurements of our samples. This work was supported by the National Advanced Material Committee of China under grant 863-715-01-02-02.

References

[1] G.B. Stringfellow, J. Crystal Growth 58 (1982) 194.
[2] G.B. Stringfellow, M.J. Cherng, J. Crystal Growth 64 (1983) 413.
[3] M.J. Cherng, H.R. Jen, C.A. Larsen, G.B. Stringfellow, J. Crystal Growth 77 (1986) 408.
[4] M.J. Cherng, G.B. Stringfellow, R.M. Cohen, Appl. Phys. Lett. 64 (1984) 677.
[5] G. Bougnot, F. Delannoy, A. Foucaran, F. Pascal, F. Roumanille, P. Grosse, J. Bougnot, J. Electrochem. Soc. 135 (1988) 1784.
[6] W.T. Tsang, T.M. Chiu, D.W. Kisker, J.A. Ditzenberger, Appl. Phys. Lett. 46 (1985) 283.
[7] R. Sankaran, G.A. Antypas, J. Crystal Growth 36 (1976) 198.
[8] E. Tournie, F. Pitard, A. Joullie, J. Crystal Growth 104 (1990) 683.
[9] T.H. Liu, J.L. Zyskind, W.T. Tsang, J. Electron. Mater. 16 (1987) 57.
[10] S.N. Iyer, A. Abul-Fadl, A.T. Macrander, J.H. Lewis, W.J. Collis, J.W. Sulhoff, Mater. Res. Symp. Proc. 160 (1990) 445.
[11] S. Iyer, S. Hegde, K.K. Bajaj, Ali. Abul-Fadl, W. Mitchel, J. Appl. Phys. 73 (1993) 3958.
[12] Zhou Tianming, Zhang Baolin, Jin Yixin, Jiang Hong, Ning Yongqiang, Rare Metals 11 (1992) 190.
[13] A.K. Srivastava, J.C. DeWinter, C. Caneau, M.A. Pollack, J.L. Zyskind, Appl. Phys. Lett. 48 (1986) 903.
[14] J.E. Bowers, A.K. Srivastava, C.A. Burrus, J.C. De Winter, M.A. Pollack, J.L. Zyskind, Electron. Lett. 22 (1986) 138.
[15] H.K. Choi, S.J. Eglash, Appl. Phys. Lett. 61 (1992) 1154.
[16] A.N. Baranov, C. Fouillant, P. Grunberg, J.L. Lazzari, S. Gaillard, A. Joullie, Appl. Phys. Lett. 65 (1994) 616.
[17] H. Lee, P.K. York, R.J. Menna, R.U. Martinelli, D.E. Garbuzor, S.Y. Narayan, J.C. Connolly, Appl. Phys. Lett. 66 (1991) 1942.
[18] Baolin Zhang, Tianming Zhou, Hong Jiang, Yixin Jin, Chemtronics 5 (1991) 149.
[19] F. Pascal, F. Delanney, J. Bougnot, L. Gouskov, G. Bougnot, P. Grosse, J. Kaoukab, J. Electron. Mater. 19 (1990) 187.
[20] Zhang Baolin, Zhou Tianming, Jiang Hong, Ning Yongqiang, Jin Yixin, Hong Chunrong, Yuan Jinshan, J. Crystal Growth 151 (1995) 21.
[21] C.A. Larson, G.B. Stringfellow, J. Crystal Growth 75 (1986) 247.
[22] G.B. Stringfellow, J. Crystal Growth 68 (1984) 111.
[23] C.P. Kuo, R.M. Cohen, K.L. Fry, G.B. Stringfellow, J. Electron. Mater. 14 (1985) 231.
[24] S.C. Chen, Y.K. Su, J. Appl. Phys. 66 (1989) 350.
[25] M.C. Wu, C.W. Chen, C.C. Chen, J. Appl. Phys. 72 (1992) 1101.
[26] G.B. Stringfellow, Organometallic Vapor-Phase Epitaxy, Academic Press, San Diego, 1989.
[27] Z.M. Fang, K.Y. Ma, R.M. Cohen, G.B. Stringfellow, Appl. Phys. Lett. 59 (1991) 1446.